

## Hidden magnetic order in $\text{Sr}_2\text{VO}_4$ clarified with $\mu^+\text{SR}$

Jun Sugiyama,<sup>1,\*</sup> Hiroshi Nozaki,<sup>1</sup> Izumi Umegaki,<sup>1</sup> Wataru Higemoto,<sup>2</sup> Eduardo J. Ansaldo,<sup>3</sup> Jess H. Brewer,<sup>3,4</sup> Hiroya Sakurai,<sup>5</sup> Ting-Hui Kao,<sup>5,6</sup> Hung-Duen Yang,<sup>6</sup> and Martin Månsson<sup>7,8</sup>

<sup>1</sup>*Toyota Central Research and Development Laboratories Incorporated, Nagakute, Aichi 480-1192, Japan*

<sup>2</sup>*Advanced Science Research Center, Japan Atomic Energy Agency, Tokai, Ibaraki 319-1195, Japan*

<sup>3</sup>*TRIUMF, 4004 Wesbrook Mall, Vancouver, British Columbia, Canada V6T 2A3*

<sup>4</sup>*Department of Physics and Astronomy, University of British Columbia, Vancouver, British Columbia, Canada V6T 1Z1*

<sup>5</sup>*National Institute for Materials Science (NIMS), 1-1 Namiki, Tsukuba, Ibaraki 305-0044, Japan*

<sup>6</sup>*Department of Physics, National Sun Yat-Sen University, Kaohsiung 804, Taiwan*

<sup>7</sup>*Laboratory for Quantum Magnetism (LQM), École Polytechnique Fédérale de Lausanne (EPFL), CH-1015 Lausanne, Switzerland*

<sup>8</sup>*Laboratory for Neutron Scattering, Paul Scherrer Institut, CH-5232 Villigen PSI, Switzerland*

(Received 17 September 2013; revised manuscript received 20 December 2013; published 6 January 2014)

In order to elucidate the magnetic ground state of  $\text{Sr}_2\text{VO}_4$ , we have measured muon spin rotation and relaxation ( $\mu^+\text{SR}$ ) spectra of a powder sample in the temperature range between 1.8 and 140 K. As a result, we have clarified that the transition at 105 K is not magnetic but structural and/or electric in origin and found the appearance of static antiferromagnetic (AF) order below 8 K. Moreover, the distribution of the internal AF field was found to be very broad, even at the lowest temperature measured. These results are consistent with the formation of an orbital-stripe order with collinear AF order for the magnetic ground state of  $\text{Sr}_2\text{VO}_4$ .

DOI: [10.1103/PhysRevB.89.020402](https://doi.org/10.1103/PhysRevB.89.020402)

PACS number(s): 75.25.Dk, 75.50.Ee, 75.70.Tj, 76.75.+i

Tetragonal  $\text{Sr}_2\text{VO}_4$  with a  $\text{K}_2\text{NiF}_4$ -type structure has been considered as an analog of a parent compound of the first superconducting cuprate, i.e.,  $\text{La}_2\text{CuO}_4$ , since the electron configuration of the  $\text{V}^{4+}$  ion is  $t_{2g}^1$  with  $S = 1/2$  in a tetragonal crystal field of a  $\text{VO}_6$  octahedron [1–7]. Although susceptibility ( $\chi_m$ ) measurements clearly show a magnetic anomaly at 105 K ( $=T_c$ ) [6], a past neutron diffraction study reported the absence of magnetic peaks even at 5 K [2]. Since x-ray diffraction studies revealed a sudden enhancement of the  $c/a$  ratio below  $T_c$  [6], it was proposed that an orbital-ordering transition occurs at  $T_c$ . In fact, first principles calculations predicted an antiferromagnetic (AF) and orbital-ordered state with a nontrivial and large unit cell structure in the ground state, because of the coexistence and competition of ferromagnetic and AF exchange interactions [8,9].

Recently, a more exciting possibility was proposed, namely, that a hidden magnetic order is induced by spin-orbit coupling for a  $t_{2g}^1$  electron system [10]. Such work also predicted an unconventional magnetic octupolar ordering at low  $T$  for  $\text{Sr}_2\text{VO}_4$ . Furthermore, alternating spin-orbital order in the  $ab$  plane was proposed by considering the effects of spin-orbit coupling, crystal field, and superexchange on the energy levels of the  $\text{V}^{4+}$  ions [11].

Despite the above attractive predictions, there are few reports on  $\text{Sr}_2\text{VO}_4$  utilizing microscopic magnetic techniques [12]. Macroscopic magnetic measurements such as  $\chi_m$  and neutron scattering usually give us significant insight into the ground state of magnetically ordered solids. However, such techniques are sometimes not suitable, particularly for the materials exhibiting order with a broad field distribution, i.e., when short-range order, random, or nearly random order appears in a material, due to the absence of periodic structure and/or the presence of rapid fluctuations. In contrast, the muon spin rotation and relaxation ( $\mu^+\text{SR}$ ) technique is very sensitive

to local magnetic environments with a different time window compared to neutron scattering; thus  $\mu^+\text{SR}$  has provided crucial information on the magnetic ground state of materials [13,14]. We have therefore performed a  $\mu^+\text{SR}$  experiment on  $\text{Sr}_2\text{VO}_4$  and found the appearance of magnetic order not below  $T_c$  but below 8 K.

A powder sample of  $\text{Sr}_2\text{VO}_4$  was prepared from a precursor orthorhombic  $\beta\text{-Sr}_2\text{VO}_4$  [15], which was made from a stoichiometric mixture of  $\text{SrO}$ ,  $\text{V}_2\text{O}_3$ , and  $\text{V}_2\text{O}_5$  by a solid state reaction at 1400 °C in an Ar gas flow for 12 h.  $\text{SrO}$  was obtained by thermal decomposition of  $\text{SrCO}_3$  at 1100 °C for 12 h under vacuum, and  $\text{V}_2\text{O}_3$  was prepared from  $\text{V}_2\text{O}_5$  by reduction in an  $\text{H}_2$  gas flow at 600 °C for 4 h, and then at 800 °C for 2 h. The obtained precursor was sealed in an Au capsule and then heated at 1300 °C under 4 GPa.

Powder x-ray diffraction (XRD) analyses revealed that the obtained sample was almost single phase of a  $\text{K}_2\text{NiF}_4$ -type structure with  $I4/mmm$  space group [2].  $\text{Sr}_3\text{V}_2\text{O}_8$  was present in the sample at a level below 2%. This suggests that the average valence of the V ion in the whole sample is above 4+, implying the absence of oxygen deficiencies in  $\text{Sr}_2\text{VO}_4$ .  $\chi_m$  ( $=M/H$ , where  $M$  is magnetization) was measured below 400 K under a  $H \leq 10$  kOe field with a superconducting quantum interference device (SQUID) magnetometer. (See Fig. 1.) A Curie-Weiss fit in the  $T$  range between 110 and 320 K provided the  $T$ -independent term [ $\chi_0 = 0.00007(2)$  emu/mol], Weiss  $T$  [ $\Theta_{\text{CW}} = -28(4)$  K], and effective magnetic moment [ $\mu_{\text{eff}} = 1.36(2)\mu_B$ ]. These values are consistent with the literature [1–5]. The  $\mu^+\text{SR}$  time spectra were measured at TRIUMF in Canada in the  $T$  range between 1.8 and 140 K. The experimental techniques are described in more detail elsewhere [13].

Figures 2(a) and 2(b) show the zero field (ZF) and longitudinal field (LF)  $\mu^+\text{SR}$  spectra at 1.8 K. Here LF means the field is parallel to the initial muon spin polarization ( $\vec{S}_\mu$ ). The ZF spectrum exhibits rapid damping with a first minimum at  $t \sim 0.25 \mu\text{s}$ , indicating the presence of a broad

\*e0589@mosk.tytlabs.co.jp

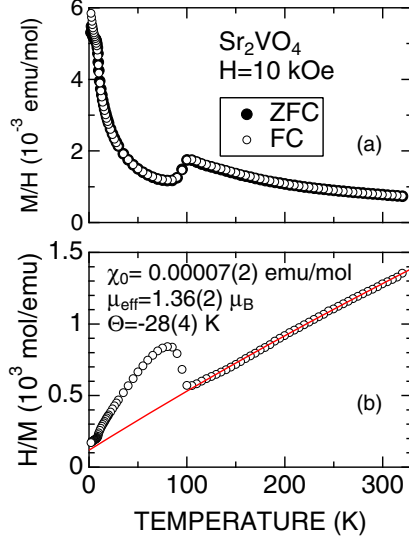


FIG. 1. (Color online)  $T$  dependence of (a) susceptibility ( $\chi_m = M/H$ ) and (b)  $1/\chi_m$  for  $\text{Sr}_2\text{VO}_4$ . The  $\chi_m$  data were obtained in field cooling (FC) mode with  $H = 10$  kOe. In (b), the red solid line represents a Curie-Weiss fit in the  $T$  range between 110 and 320 K.

distribution of internal fields ( $H_{\text{int}}$ ). Since the LF clearly decouples the damping, the ZF and LF spectra are likely to be fitted by a dynamic Gaussian Kubo-Toyabe function ( $G_{\text{KT}}$ ) due to random  $H_{\text{int}}$ 's at the muon sites [16]. However, two additional exponentially relaxing signals are required in order to reproduce the spectra, that is,

$$A_0 P(t) = A_{\text{KT}} G_{\text{KT}}(\Delta, \nu_{\text{fluct}}, t, H_{\text{LF}}) + A_{\text{F}} e^{-\lambda_{\text{F}} t} + A_{\text{S}} e^{-\lambda_{\text{S}} t}, \quad (1)$$

where  $A_0$  is the initial asymmetry,  $P(t)$  is the muon spin depolarization function,  $A_{\text{KT}}$ ,  $A_{\text{F}}$ , and  $A_{\text{S}}$  are the asymmetries associated with the three signals,  $G_{\text{KT}}(\Delta, 0, t, 0) = 1/3 + 2/3(1 - \Delta^2 t^2) \exp(-\Delta^2 t^2/2)$ ,  $\Delta$  is the field distribution width at the muon site,  $\nu_{\text{fluct}}$  is the fluctuation rate of the local fields responsible for  $G_{\text{KT}}$ , and  $\lambda_{\text{F}}$  and  $\lambda_{\text{S}}$  are the exponential relaxation rates.

A global fit for the spectra at 1.8 K [see Fig. 2(a)], in which we used common parameters in Eq. (1) for the ZF and two-LF spectra, yielded  $A_{\text{KT}} = 0.096(3)$  with  $\Delta = 7.8(2) \mu\text{s}^{-1}$  and  $\nu_{\text{fluct}} = 0.41(2) \mu\text{s}^{-1}$ ,  $A_{\text{F}} = 0.081(7)$  with  $\lambda_{\text{F}} = 20(2) \mu\text{s}^{-1}$ , and  $A_{\text{S}} = 0.036(5)$  with  $\lambda_{\text{S}} = 3.2(5) \mu\text{s}^{-1}$ . This implies the presence of three different muon sites in the lattice, whereas there is only one muon site in the isostructural compound  $\text{La}_2\text{CuO}_4$  [17]. Also, since  $\nu_{\text{fluct}} \ll \Delta$ ,  $H_{\text{int}}$  at the site responsible for the  $A_{\text{KT}}$  signal is almost static, while those for the other two sites are dynamic even at 1.8 K. This is an inconsistent situation, even though the three sites are crystallographically equivalent, but magnetically nonequivalent.

In order to obtain acceptable results for a *single* muon site, the ZF spectra were finally fitted by a combination of an exponentially relaxing cosine oscillation for the quasistatic internal field and an exponentially relaxing nonoscillatory signal for the “1/3 tail” signal caused by fluctuations in the

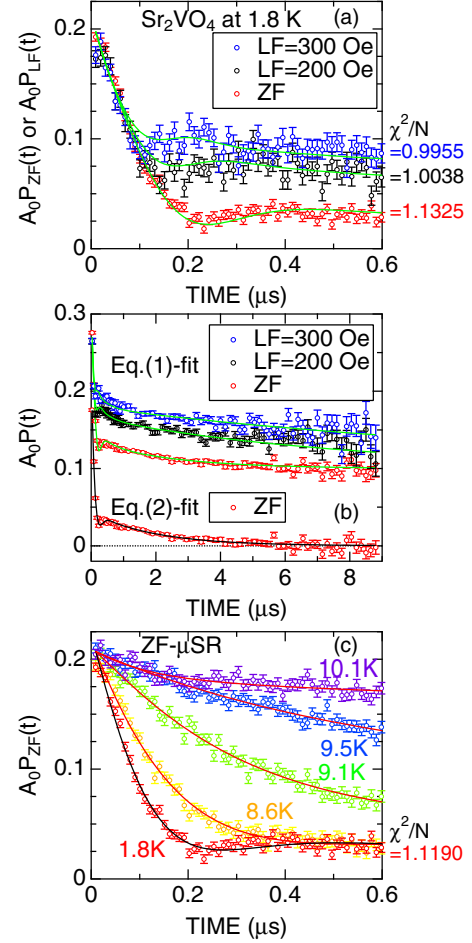


FIG. 2. (Color online) The ZF and LF  $\mu^+$ SR spectrum in  $\text{Sr}_2\text{VO}_4$  obtained at 1.8 K (a) in an early time domain and (b) in the whole time domain measured; (c) the variation of the ZF  $\mu^+$ SR spectrum with  $T$ . Solid green lines in (a) and (b) represent the fit result using Eq. (1) and its analog for LF, while solid black and red lines in (b) and (c) represent that using Eq. (2). In (b), the  $\mu^+$ SR spectra and fit result using Eq. (1) are shifted by 0.1 for clarity of display. Since the fit was performed to minimize  $\chi^2$ , reduced  $\chi^2$  ( $=\chi^2/N$ ) for the data at 1.8 K is shown for comparison, where  $N$  is degree of freedom.

field component parallel to  $\vec{S}_\mu$ :

$$A_0 P_{\text{ZF}}(t) = A_{\text{AF}} e^{-\lambda_{\text{AF}} t} \cos(\omega_{\text{AF}}^\mu t) + A_{\text{tail}} e^{-\lambda_{\text{tail}} t}, \quad (2)$$

where  $f_{\text{AF}} (\equiv \omega_{\text{AF}}^\mu/2\pi)$  is the muon Larmor frequency corresponding to the AF quasistatic  $H_{\text{int}}$ ,  $A_{\text{AF}}$  and  $A_{\text{tail}}$  are the asymmetries of the two signals, and  $\lambda_{\text{AF}}$  and  $\lambda_{\text{tail}}$  are their exponential relaxation rates. Moreover,  $A_0 = 0.226 (=A_{\text{AF}} + A_{\text{tail}})$ , which is the full asymmetry, is fixed in the whole  $T$  range below 25 K, based on weak transverse field (WTF) data at 80 K. Here we should note again that both equations represent the same physical description, i.e., the presence of quasistatic  $H_{\text{int}}$  with broad distributions.

Figure 3 shows the  $T$  dependences of the  $\mu^+$ SR parameters together with  $\chi_m$  measured at  $H = 10$  and 100 Oe. We also plot the WTF asymmetry ( $A_{\text{TF}}$ ), which monitors the nonmagnetic volume fraction in the sample, as described later. As  $T$  increases from the lowest  $T$  measured (1.8 K),  $A_{\text{AF}}$  is almost

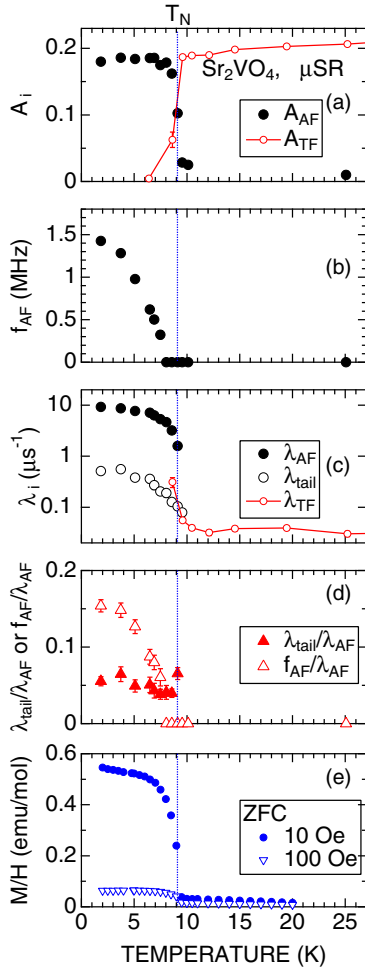


FIG. 3. (Color online)  $T$  dependences of (a) the asymmetries ( $A_{\text{AF}}$  and  $A_{\text{TF}}$ ), (b) the muon spin precession frequency for the  $A_{\text{AF}}$  signal ( $f_{\text{AF}}$ ), (c) the exponential relaxation rates  $\lambda_{\text{AF}}$ ,  $\lambda_{\text{tail}}$ , and  $\lambda_{\text{TF}}$ , (d) the ratio between  $\lambda_{\text{tail}}$  and  $\lambda_{\text{AF}}$  as well as  $f_{\text{AF}}$  and  $\lambda_{\text{AF}}$ , respectively, and (e)  $\chi_m$  ( $=M/H$ ) for  $\text{Sr}_2\text{VO}_4$ . The  $\chi_m$  data were obtained in a zero field cooling (ZFC) mode with  $H = 10$  and  $100$  Oe. The WTF data is the same to that in Fig. 4.

$T$  independent ( $A_{\text{AF}} \sim 0.18$ ) until  $8$  K, and then suddenly drops to  $\sim 0.02$  and becomes  $T$  independent again until  $25$  K. Meanwhile, as  $T$  decreases from  $25$  K,  $A_{\text{TF}}$  is roughly  $T$  independent above  $9$  K, and then rapidly decreases down to  $\sim 0$  below  $9$  K. The  $A_{\text{AF}}(T)$  and  $A_{\text{TF}}(T)$  curves suggest that  $T_N = 9.2$  K, at which  $A_{\text{AF}}/A_0 = A_{\text{TF}}/A_0 \sim 0.5$ .

On the contrary, as  $T$  increases from  $1.8$  K,  $f_{\text{AF}}$  decreases with increasing slope  $df_{\text{AF}}/dT$  and disappears at  $\sim 8$  K. Although  $T_N = 9.2$  K by the asymmetry data, the oscillatory signal, which indicates the formation of static long-range magnetic order, disappears above  $8$  K due to the large relaxation of a signal below the vicinity of  $T_N$ .

The two relaxation rates ( $\lambda_{\text{AF}}$  and  $\lambda_{\text{tail}}$ ) exhibit a  $T$  dependence similar to that for  $f_{\text{AF}}$  below  $T_N$ . In fact, the ratio  $\lambda_{\text{tail}}/\lambda_{\text{AF}}$  is also  $T$  independent below  $T_N$ , confirming the same origin for the two signals. Although  $A_{\text{tail}}$  is only  $\sim 22\%$  of  $A_0$ , such  $T$  dependence of  $\lambda_{\text{tail}}$  is reasonable for the “1/3 tail” signal. The smaller  $A_{\text{tail}}$  is probably due to the coexistence of a spin-glass-like phase, which provides no “1/3 tail” signal. By

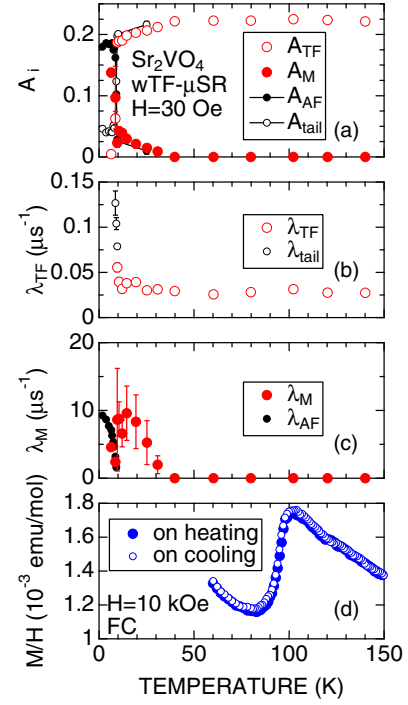


FIG. 4. (Color online)  $T$  dependences of (a) the two asymmetries,  $A_{\text{TF}}$  and  $A_{\text{M}}$ , their exponential relaxation rates (b)  $\lambda_{\text{AF}}$  and (c)  $\lambda_{\text{M}}$ , and (d)  $\chi_m$  ( $=M/H$ ) for  $\text{Sr}_2\text{VO}_4$ . The data in (a)–(c) were obtained by fitting WTF  $\mu^+\text{SR}$  spectra using Eq. (3). In (a)–(c), the ZF  $\mu^+\text{SR}$  parameters,  $A_{\text{AF}}$ ,  $A_{\text{tail}}$ ,  $\lambda_{\text{tail}}$ , and  $\lambda_{\text{AF}}$ , are also plotted for comparison.

contrast, the ratio  $f_{\text{AF}}/\lambda_{\text{AF}}$ , which corresponds to the inverse of the field distribution normalized to  $H_{\text{int}}$ , decreases with  $T$  and approaches zero at  $T_N$ , as expected. We wish to emphasize that, since  $\lambda_{\text{AF}}/\omega_{\text{AF}} \sim 1$  even at  $1.8$  K, the magnetic order in  $\text{Sr}_2\text{VO}_4$  is different from a usual long-range AF order, for which  $\lambda_{\text{AF}}/\omega_{\text{AF}} \ll 1$ .

Such a broad field distribution is more likely to support orbital-stripe order and collinear AF spin order [8,9] rather than alternating spin-orbital order [11]. This is because, even for the single muon site in the lattice, dipole field calculations showed that there are several  $H_{\text{int}}$ 's in the former case, while only one well defined  $H_{\text{int}}$  would be expected in the latter case.

Finally, the  $\chi_m(T)$  curve obtained with  $H = 10$  Oe indicates a clear increase below  $T_N$ , in addition to the remarkable anomaly around  $105$  K. The present work clearly demonstrates that the bulk magnetic transition does not occur at  $105$  K but at  $9.2$  K for  $\text{Sr}_2\text{VO}_4$ .

In order to study the change in local magnetic environments at  $T_c = 105$  K, Fig. 4 shows the  $T$  dependences of the fitted  $\mu^+\text{SR}$  parameters obtained from WTF measurements with  $H_{\text{TF}} = 30$  Oe, together with the ZF  $\mu^+\text{SR}$  parameters. Here, WTF means that  $\vec{H}_{\text{TF}} \perp \vec{S}_\mu$  and  $|H_{\text{TF}}| \ll |H_{\text{int}}|$ . The WTF spectra were fitted by

$$A_0 P_{\text{TF}}(t) = A_{\text{TF}} \cos(\omega_{\text{TF}}t + \phi) e^{-\lambda_{\text{TF}}t} + A_{\text{M}} e^{-\lambda_{\text{M}}t}, \quad (3)$$

where  $A_{\text{TF}}$  and  $A_{\text{M}}$  are the asymmetries for the oscillatory signal due to applied WTF and the nonoscillatory relaxing signal caused by localized magnetic moments.

From the  $A_{\text{TF}}(T)$  curve in Fig. 4(a), the whole volume of the sample is found to be paramagnetic above 40 K, as shown in Fig. 3(a). Although the  $\lambda_{\text{TF}}(T)$  curve, which corresponds to the spin-spin relaxation rate, seems to show a small maximum around 100 K, this feature is obviously not magnetic but rather structural and/or electric in origin. The anomaly in the  $\chi_{\text{m}}(T)$  curve at  $T_{\text{c}}$  is thus likely to show the formation of a spin-singlet-like state, as for other vanadium oxides, e.g.,  $\text{V}_4\text{O}_7$  (Refs. [18,19]) and  $\text{K}_2\text{V}_8\text{O}_{16}$  [20–22]. A slight structural change in  $\text{Sr}_2\text{VO}_4$  (Ref. [6]) would result in a V dimerization creating the spin singlets that manifest themselves as a drastic decrease in  $\chi_{\text{m}}$  at  $T_{\text{c}}$ .

Concerning the  $T$  range below 50 K, as  $T$  decreases from 50 K,  $A_{\text{M}}$  first appears below 40 K and increases monotonically with decreasing  $T$ , while  $A_{\text{TF}}$  starts to decrease below 40 K. This indicates the evolution of localized magnetic moments with decreasing  $T$  and might imply the formation of short-range order in the  $T$  range between 40 K and  $T_{\text{N}}$ , similarly to other low-dimensional systems, such as  $[\text{Ca}_2\text{CoO}_3]_{0.62}[\text{CoO}_2]$  (Ref. [23]) and  $\text{Ca}_3\text{Co}_2\text{O}_6$  [24]. This behavior is most unlikely to be caused by inhomogeneity but highly likely an intrinsic

feature of  $\text{Sr}_2\text{VO}_4$ . Therefore, it is highly desirable to perform careful inelastic neutron scattering studies in this  $T$  range. Finally, at  $T_{\text{N}}$ ,  $A_{\text{TF}}$  drops to zero due to the formation of magnetic order, as seen in the ZF measurements [Fig. 3(b)].

In summary, we have investigated the magnetic nature of  $\text{Sr}_2\text{VO}_4$  with  $\mu^+\text{SR}$  and found the formation of static long-range AF order below 8 K, although the field distribution is very broad even at 1.8 K. By contrast, the transition at  $T_{\text{c}} = 105$  K was found to be not magnetic. This naturally leads to a question on the recent theoretical work, in which the spin-orbit coupling plays a significant role in the magnetic ground state of  $\text{Sr}_2\text{VO}_4$ . This is because  $T_{\text{N}} \ll T_{\text{c}}$ , at which orbital ordering is proposed to occur [6,10,11].

We thank the staff of TRIUMF for help with the  $\mu^+\text{SR}$  experiments. This work was supported by MEXT KAKENHI Grant No. 23108003. H.S. was supported by the FIRST Program of JSPS. T.K. was supported by the NIMS internship program. H.D.Y. was supported by National Science Council of Taiwan. M.M. was supported by SNSF and its *Sinergia* network “Mott Physics Beyond the Heisenberg Model.”

- 
- [1] M. Rey, P. Dehault, J. Joubert, B. Lambert-Andron, M. Cyrot, and F. Cyrot-Lackmann, *J. Solid State Chem.* **86**, 101 (1990).
- [2] M. Cyrot, B. Lambert-Andron, J. Soubeyroux, M. Rey, P. Dehault, F. Cyrot-Lackmann, G. Fourcaudot, J. Beille, and J. Tholence, *J. Solid State Chem.* **85**, 321 (1990).
- [3] M. Itoh, M. Shikano, H. Kawaji, and T. Nakamura, *Solid State Commun.* **80**, 545 (1991).
- [4] A. Nozaki, H. Yoshikawa, T. Wada, H. Yamauchi, and S. Tanaka, *Phys. Rev. B* **43**, 181 (1991).
- [5] N. Suzuki, T. Noritake, and T. Hioki, *Mater. Res. Bull.* **27**, 1171 (1992).
- [6] H. D. Zhou, B. S. Conner, L. Balicas, and C. R. Wiebe, *Phys. Rev. Lett.* **99**, 136403 (2007).
- [7] R. Viennois, E. Giannini, J. Teyssier, J. Elia, J. Deisenhofer, and D. V. der Marel, *J. Phys.: Conf. Ser.* **200**, 012219 (2010).
- [8] Y. Imai, I. Solovyev, and M. Imada, *Phys. Rev. Lett.* **95**, 176405 (2005).
- [9] Y. Imai and M. Imada, *J. Phys. Soc. Jpn.* **75**, 094713 (2006).
- [10] G. Jackeli and G. Khaliullin, *Phys. Rev. Lett.* **103**, 067205 (2009).
- [11] M. V. Eremin, J. Deisenhofer, R. M. Eremina, J. Teyssier, D. van der Marel, and A. Loidl, *Phys. Rev. B* **84**, 212407 (2011).
- [12] K. Yamauchi, M. Miyazaki, M. Hiraiishi, A. Koda, K. Kojima, R. Kadono, K. Nawa, H. Ueda, K. Yoshimura, and H. Takigawa, in Abstracts of the Autumn Meeting of Phys. Soc. Jpn., 2013 (unpublished).
- [13] G. M. Kalvius, D. R. Noakes, and O. Hartmann, in *Handbook on the Physics and Chemistry of Rare Earths*, Vol. 32 (North-Holland, Amsterdam, 2001) Chap. 206, pp. 55–451.
- [14] A. Yaouanc and P. D. de Réotier, *Muon Spin Rotation, Relaxation, and Resonance, Application to Condensed Matter* (Oxford University Press, New York, 2011).
- [15] W. Gong, J. Greedan, G. Liu, and M. Bjorgvinsson, *J. Solid State Chem.* **95**, 213 (1991).
- [16] R. S. Hayano, Y. J. Uemura, J. Imazato, N. Nishida, T. Yamazaki, and R. Kubo, *Phys. Rev. B* **20**, 850 (1979).
- [17] S. B. Sulaiman, S. Srinivas, N. Sahoo, F. Hagelberg, T. P. Das, E. Torikai, and K. Nagamine, *Phys. Rev. B* **49**, 9879 (1994).
- [18] A. C. Gossard, J. P. Remeika, T. M. Rice, H. Yasuoka, K. Kosuge, and S. Kachi, *Phys. Rev. B* **9**, 1230 (1974).
- [19] Y. Ueda, Y. Kitaoka, H. Yasuoka, K. Kosuge, and S. Kachi, *J. Phys. Soc. Jpn.* **47**, 333 (1979).
- [20] M. Isobe, S. Koishi, N. Kouno, J.-I. Yamaura, T. Yamauchi, H. Ueda, H. Gotou, T. Yagi, and Y. Ueda, *J. Phys. Soc. Jpn.* **75**, 073801 (2006).
- [21] Y. Shimizu, K. Okai, M. Itoh, M. Isobe, J.-I. Yamaura, T. Yamauchi, and Y. Ueda, *Phys. Rev. B* **83**, 155111 (2011).
- [22] K. H. Chow, M. Månsson, Y. Ikedo, J. Sugiyama, O. Ofer, E. J. Ansaldo, J. H. Brewer, M. Isobe, H. Gotou, T. Yagi *et al.*, *Phys. Procedia* **30**, 117 (2012).
- [23] J. Sugiyama, H. Itahara, T. Tani, J. H. Brewer, and E. J. Ansaldo, *Phys. Rev. B* **66**, 134413 (2002).
- [24] J. Sugiyama, H. Nozaki, Y. Ikedo, K. Mukai, D. Andreica, A. Amato, J. H. Brewer, E. J. Ansaldo, G. D. Morris, T. Takami *et al.*, *Phys. Rev. Lett.* **96**, 197206 (2006).